SLOPE STABILITY ANALYSIS, REVISITED

INTRODUCTION

In the early days of my engineering career Stability Analyses were computed by hand calculation and were tedious, but nevertheless were a requirement for even small dams. So, for the handful of potential sliding surfaces which could be examined a great deal of thinking went into deciding where might be the weaknesses in the design section. And that contemplation was in my opinion more important than whatever safety factor came out of the calculations. Of course all that changed with the advent of computers and search routines.

While I was an enthusiastic user of computers, writing several of my own programs for stability computations, it became apparent to me that something was missing. This was especially so when it came to "end of construction" and "upstream rapid drawdown" pore pressure conditions. More recently the relatively straightforward "steady state seepage" condition for the downstream slope became worrisome, particularly in the light of the experiences at Tarbela and Bennett dams. Perhaps, I thought, it is time to take a fresh look at the prevailing notions about how the soil-structure actually behaved in the presence of energized water; taking for granted what seems evident, that - where there is no water there is no problem.

What is presented here is a "start from scratch" examination of the forces at play within a soil slope affected by seepage water. I find forces more tangible than stresses or pressures. When it comes to the all-important quantification of pore water pressures, this scalar quantity seems rather ethereal compared with a force vector which defines both magnitude and direction of action. Vectors can be drawn and resolved as a force polygon; this graphical representation of forces ensures that all vectors are apparent. And once the polygon closes we gain some confidence that we are doing the right thing. In consequence, examination of forces, as opposed to pressures or stresses, is adopted as the guiding principle on which this approach is founded.

COMPUTATIONAL PROCEDURE

This new approach to assessing the stability of slopes is labeled the hydrodynamic method (h-method). It differs from existing methods in that it recognizes, and deals with, the hydraulic energy dissipated within a water retaining embankment. In order to appreciate the need for this change in computation it is only necessary to realize that had there been no dam at this location, then there would have been a waterfall: and in that case the energy in the falling water would have been expended in forming a plunge pool.

As is common practice, the "method of slices" is employed here as a convenient means of distributing effective overburden weights to underlying sections of the trial

failure surface. Since the boundaries of these imaginary slices have no real existence, no consideration is given to inter-slice forces.

Figure 1 shows the slope geometry which will herein be examined under various soil-structure and hydraulic constraints. It is a 2:1 granular fill embankment, and as shown there, founded on a cohesive deposit. The differential head between the pond level and the tailwater results in seepage flow through the soils.

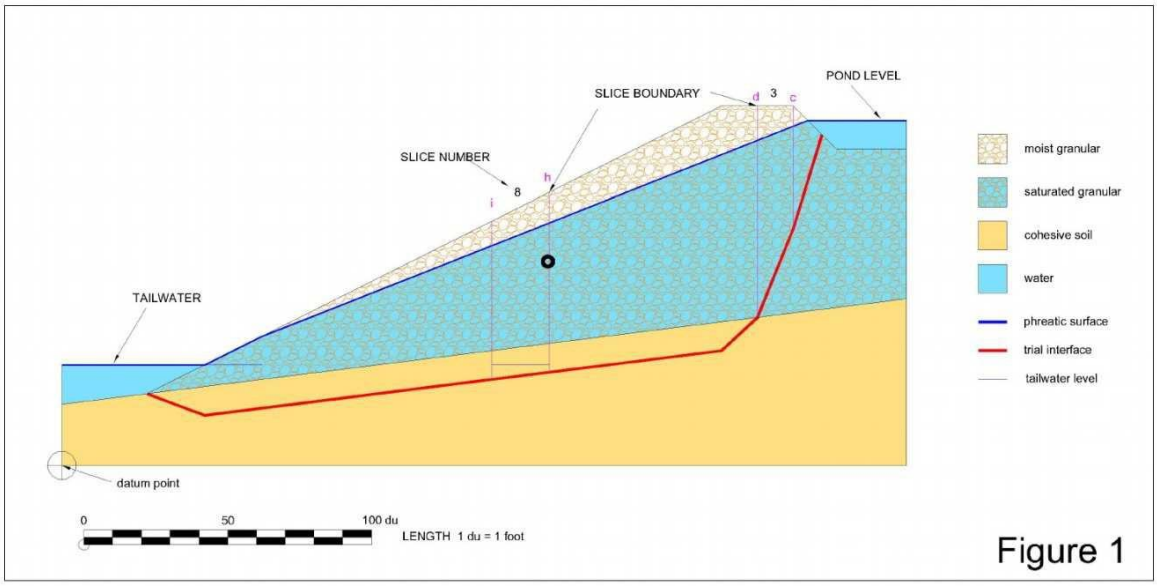

Figure 1

The black donut shows the centre of mass (effective) of the soils above the trial interface. The foot-pound system of units is used here. Following convention, volumes are taken as being numerically equal to surface areas on the understanding that thicknesses are of unit depth.

Figures 2 and 3 show the physical conditions associated with Slices 3 and 8, respectively. There are two sketches on each figure: The one on the left side depicts the solid soil-structure forces and the pressures from which these are derived; the one on the right deals with the liquid phase - pore water. These two intimately related phases of the soil will be examined separately before combining their influence on stability. First, the solid phase:

Solids of soil-structure

Here the phreatic surface is used to discriminate between the moist soil above and the saturated soil below. The moisture content above is set at the equivalent of 5% saturation, see Ref 1. Soils below the phreatic line are considered fully saturated, and consequently exert only their buoyant weight on the soil-structure beneath.

This is consistent with standard usage as in the equation for shear strength:

$$s = c + (\sigma_n - u) \tan \Phi$$

where the parenthetical term is equivalent to the sense used here.

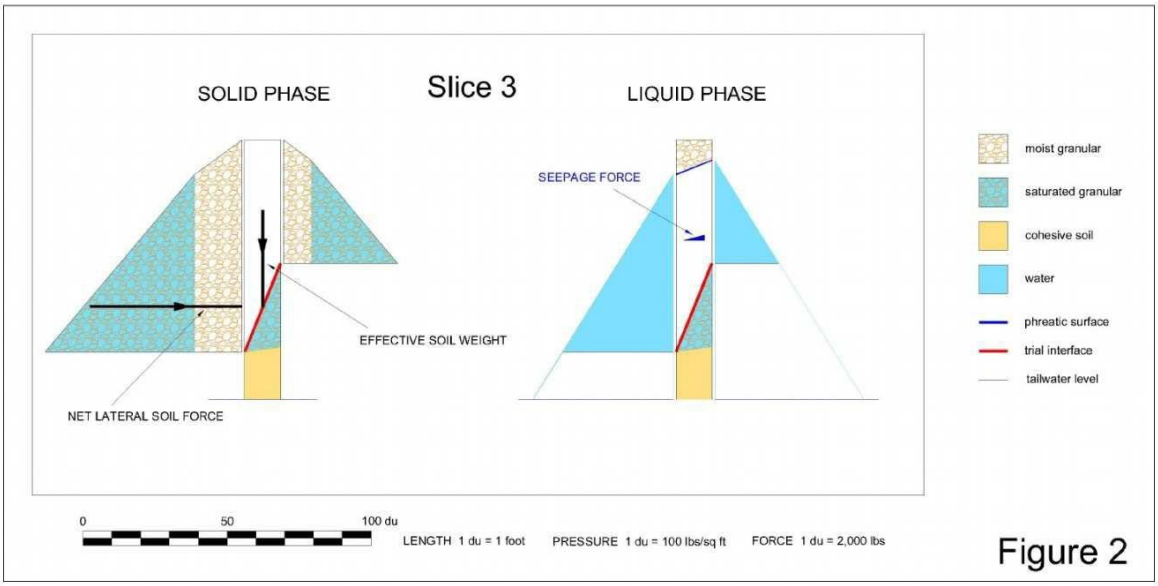

Figure 2

The resultant vertical force acting on the trial interface is shown to scale, as is the resultant of the horizontal force brought about by lateral soil pressures on the two vertical sides of the slice.

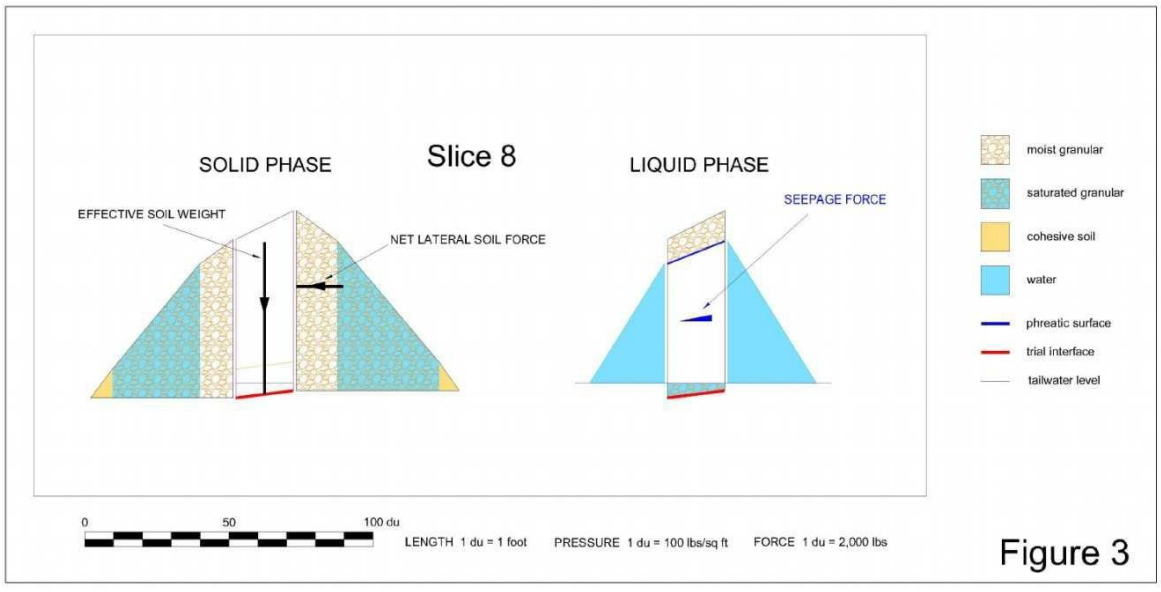

Figure 3

Figure 4 shows the force polygons for Slices 3 and 8 as derived from Figures 2 and 3.

These latter forces are of no consequence to stability since over the length of the stability section these obviously balance out, and all that remains is the difference in hydraulic/hydrostatic force between the first and last slices. They are only drawn here to indicate the relative magnitudes of the forces involved, and also make it apparent that they have not been ignored.

The two force magnitudes of interest here are:

a. P, the component of the effective soil weight (W') parallel to the base of the slice, from which we find "H", the force which depends upon the inclination of the interface, and

b. S, the ultimate shear resistance to translation along the base.

These two pieces of information from each of the slices, together with the knowledge that inter-slice lateral forces cancel out, we have learned all that is relevant to stability from the solid phase geometry.

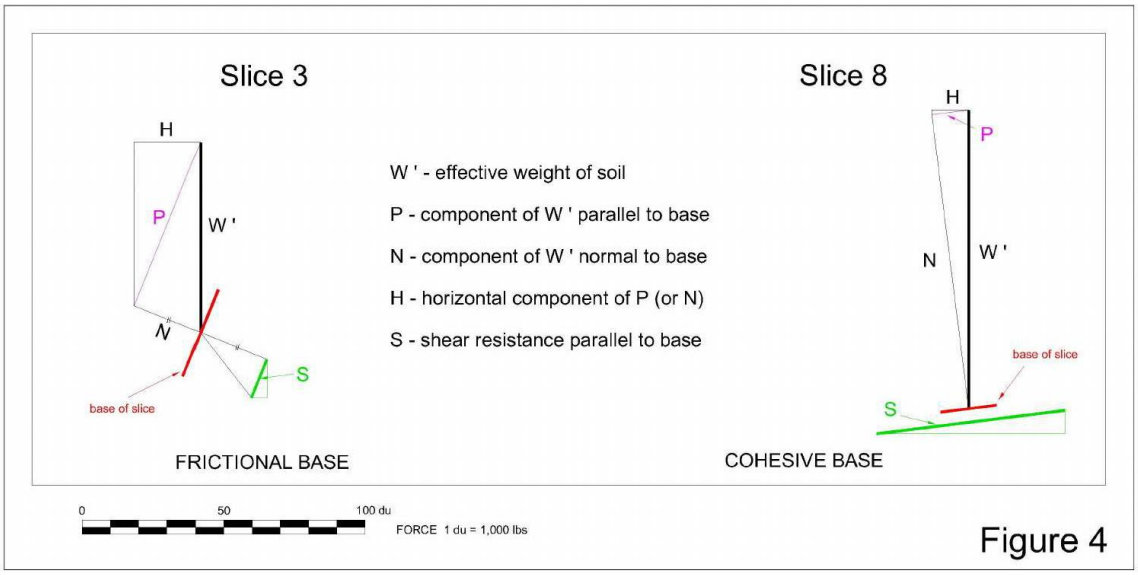

Figure 4

The methodology underlying this analytical approach is to treat the mass above the trial interface as a "free-body", that is to say, only boundary restraints to movement, and forces emanating from within the body itself need be considered in order to establish its stability with respect to translation along the interface.

Now that we have accounted for the solid phase, we must next consider the liquid phase. The fact that steady state seepage is occurring within the soil-structure, a persistent event which leads to energy being expended within the system, is a reality which must next be granted the special attention and consideration it demands.

Water within the soil-structure

To establish that steady state seepage is an important component of slope stability it is only necessary to appreciate what is shown in Figure 5.

This photograph taken through the glass wall of a water filled test tank, see Ref 2. The water level is indicated by the hand-drawn arrow near the upper right-hand corner. Clean sand was placed loosely within a cylindrical latex membrane. A drainage layer of fine crushed rock (the lighter color) underlay the sandfill. This drain was vented to the atmosphere by a vertical outlet. Then, after submergence within the tank, the membrane was gradually pulled up to expose the sandfill directly to the surrounding water. The dry (subaerial) angle of repose of this sand is 34°. Here it may be seen to stand with a vertical side slope underwater. The reason for this counterintuitive behavior is the creation of an inward hydraulic gradient due to the differential radial water pressures, in other words, a phreatic surface inclined from the sand face to the inner drain.

Figure 5

Obviously, this real and powerful phenomenon ought to be made part of stability analyses computations.

SEEPAGE FORCES

The essential starting point in appreciation Seepage Forces [**SF**] is the realization that pore water pressures, when quiescent/hydrostatic, have no influence whatever on the buoyant soil-structure: It is only pore pressure gradients that affect the soil-structure, and thereby a slope's stability. The inclination of the phreatic surface is

simply the maximum hydraulic gradient prevailing within the saturated soils beneath. As our attention moves down through the sub-parallel flow lines lower down the slice, the value of the gradient decreases gradually, until becoming zero at tailwater level.

In Figure 6 we can see how a dissipating phreatic surface may be interpreted and translated into a SF, such as those responsible for the vertical slopes in Figure 5. The diagram on the left of Figure 6 shows the hydraulic conditions that prevail in the liquid phase, using Slice 8 of Figure 1 as a typical case in point. The box to the right shows the relationship between the volume of the saturated soil within the slice (V), and the water pressures encompassing it, can be expressed as a single hydraulic vector effecting that particular slice.

We may now write an equation quantifying the SF acting within any slice in terms of the variables we know:

$$SF = i \ \gamma_w \ V \qquad \text{Equation 1}$$

Where the first term is the average hydraulic gradient [***i***] prevailing within the saturated soils; γ_w is the unit weight of water, and V is the volume (area of unit thickness) subject to flow.

What may require some further elucidation is why, and how, SF could become attached to, and affect, the soil-structure phase. And that is explained as follows: In a porous medium such as earthfill, if there is an inclination to the phreatic surface, water will flow in the direction of the maximum downward gradient (flow line). The rate of flow will be in accordance with D'Arcy's Law, where *k* (permeability or hydraulic conductivity) is the resistance to flow, a measure of the energy requirements to sustain it.

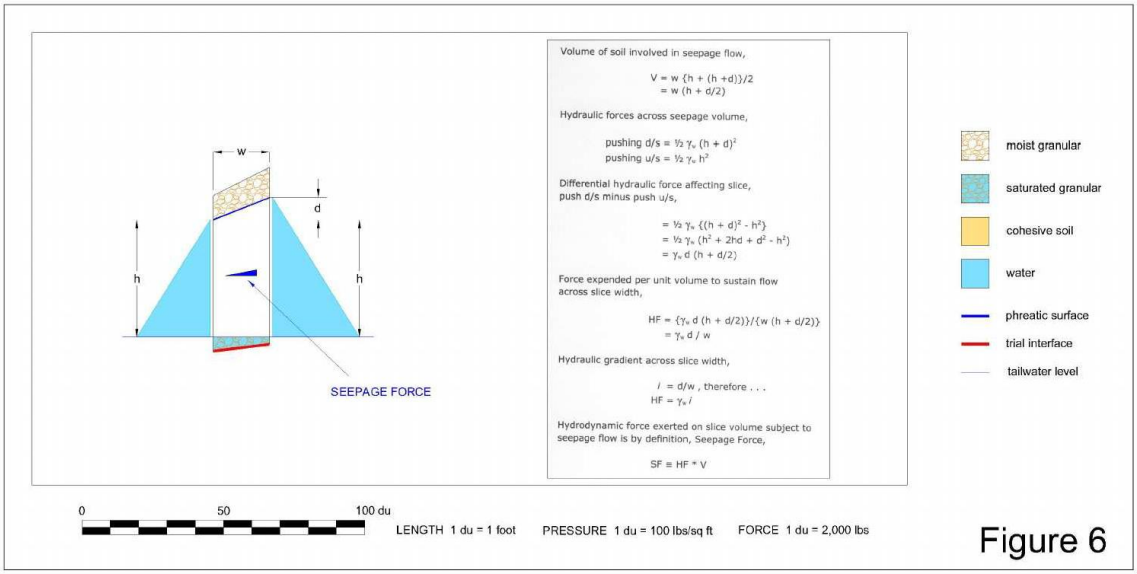

Figure 6

If we now switch our perspective from the water to the soil-structure, that is, from energy expended to work done, we are led to ask the question: What is the work done on? And this is where our sister discipline, Fluid Mechanics, gives us the answer. The work is done in overcoming the hydrodynamic Drag Force [$\mathbf{D_F}$] which resists the relative motion of water past the solids. D_F is proportional to the square of the relative velocity, and is composed of frictional and viscous elements.

A detailed quantification of this exchange of energy is given in Ref 3**.**

This force is calculated using their equation:

$$F_D = C_D \rho A v^2 / 2,$$

where,

C_D	Coefficient of Drag
ρ	mass density of fluid
A	equatorial area of the solid
v	relative velocity of fluid and solid.

Relevance of Seepage to Stability

The phreatic surface is the locus of the level to which water would rise in a standpipe installed in the embankment. That piezometric elevation is the measure of the total hydraulic energy in the water beside the porous tip. This is called the hydraulic head above the monitored point and is the sum of the potential/pressure energy and the kinetic/velocity energy in that water. Its magnitude is usually quoted as a length (feet or meters).

If the phreatic surface is flat across the area of interest, as in Figure 7, then there is no differential in hydraulic energy within that field. Consequently, there can be no flow, because moving water needs energy to support the effort of working its way through the warren that is the soil-structure. This condition we call hydrostatic.

So, in practical terms what happens during steady state seepage through a porous media is that the water, in seeking tailwater level, tends to drag the soil- structure in the same direction. In doing so it transfers by frictional and viscous drag forces, energy to the soil-structure, and this, as an intergranular compression parallel to the flow lines. This give-and-take between the fluid phase (seepage water) and the solid phase (soil-structure), from the point of view of Stability Analysis [**SA**], has two effects:

c. The horizontal component (SF_H) is a destabilizing influence.

d. On the other hand, the vertical component (SF_V), is a stabilizing influence in that it adds to the effective normal force on a sandy trial sliding interface, the shear resistance in granular soils is increased, but brings no similar benefit to soil sections where the base soils are cohesive.

The hypotenuse of the solid blue triangle is centered on the point of action and is drawn to scale. The orthogonal sides represent the horizontal (SF_H) and vertical (SF_V) components of SF. So we may now return to the diagrams on the right side of Figures 2 and 3 and appreciate what they portray.

Equation 1 was used to calculate the seepage forces for each of the 14 slices for their particular geometry and phreatic situation as depicted in Figure 1. The cumulative magnitudes of these force resultants are shown graphically on Figures 7, 8 and 9 which depict the three phreatic surfaces which were chosen for comparative study here.

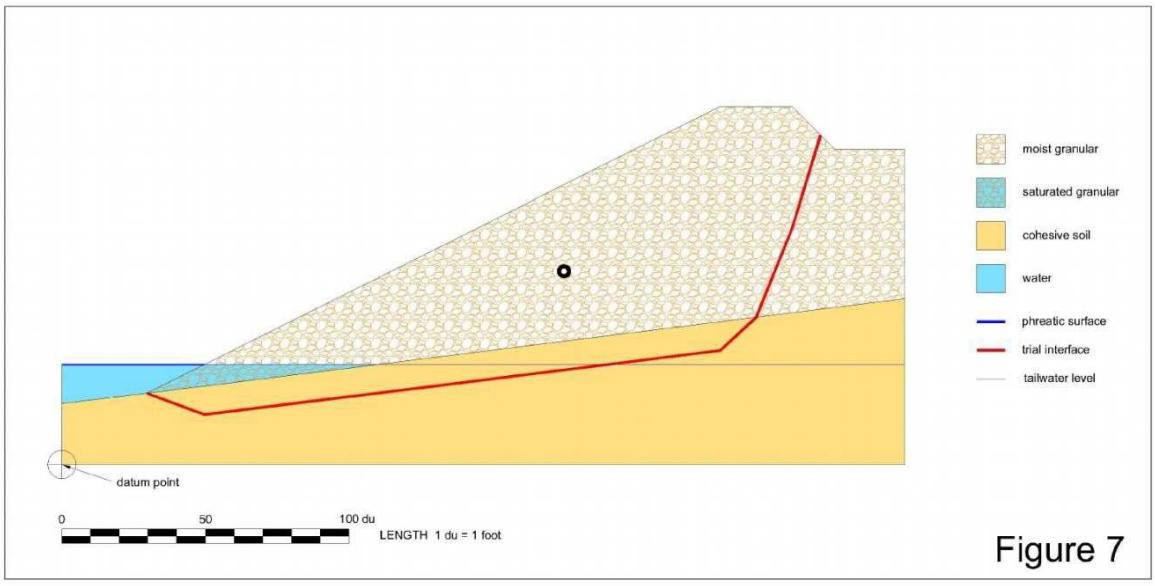

Figure 7

Figure 7 shows a blank in this regard because there is no gradient to the phreatic surface and consequently there is no seepage flow.

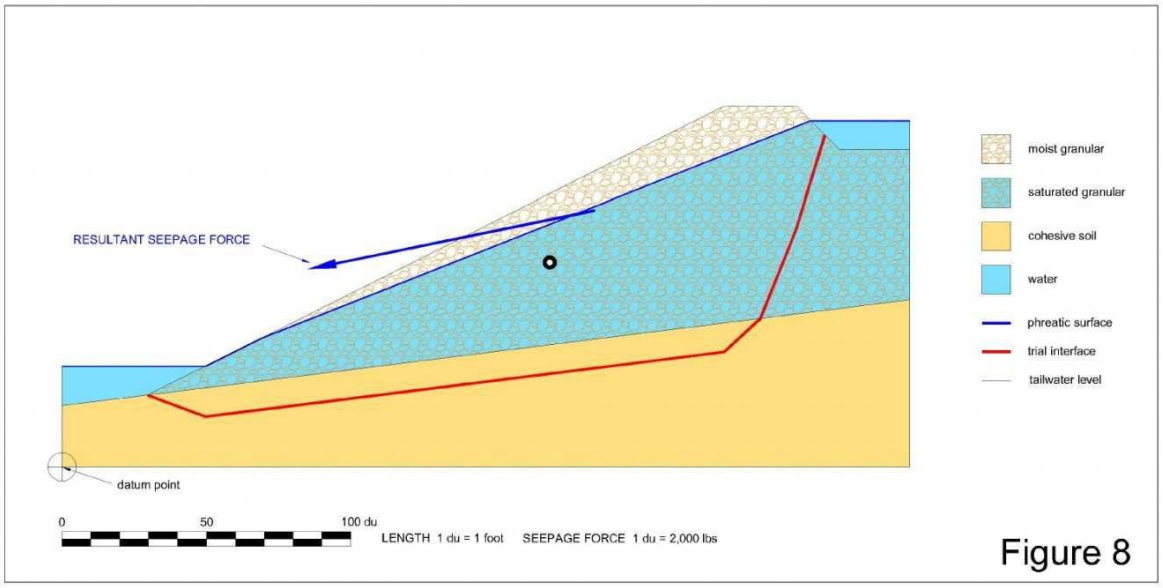

Figure 8, on the other hand, shows a full pool, and a phreatic surface in the earthfill with no provision such as drainage in the downstream [**d/s**] shell to impede its full expression. The inclined blue line represents the SF to scale: The tail end of the vector is set at the point where its centre of origin is located.

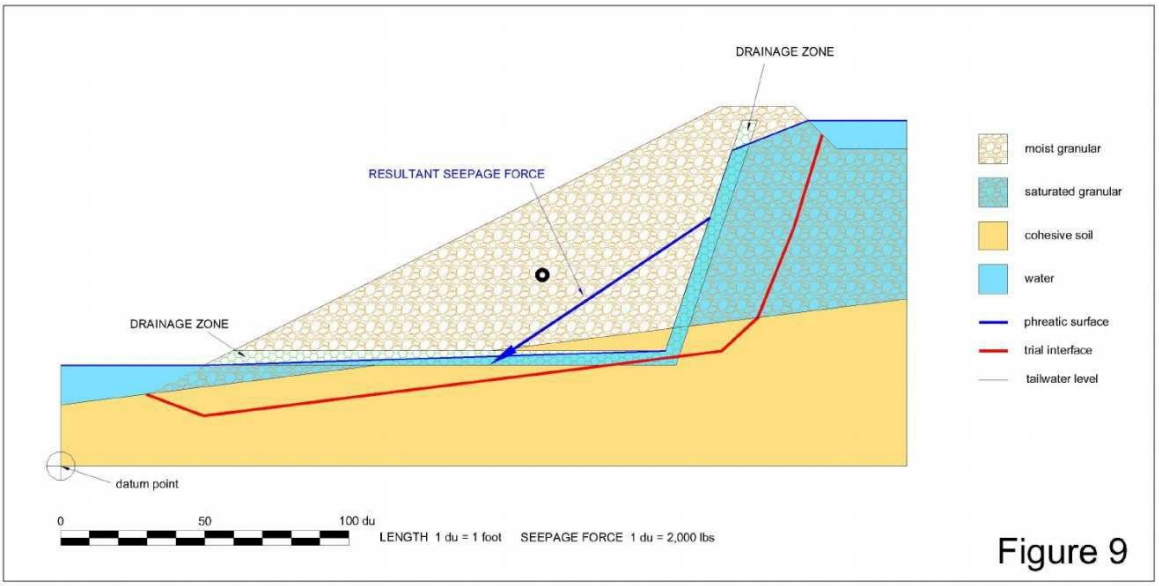

Figure 9 also represents a full pool, however, in this case the phreatic surface is depressed by a chimney drain relieved/connected to a toe drain: theoretically the optimal way to minimize SFs within the d/s shell. As can be seen, that vector has been kept well within the earthworks' profile.

Table 1, below, lists the numerical values of these SF force components.

FACTOR OF SAFETY

Definition

As is appropriate for the non-circular trial failure interface being considered here, I have chosen to define Factor of Safety [**FoS**] in terms of the ratio of horizontal forces: These being the ratio of shear forces resisting horizontal movement of the mass above the trial interface, to those soil-structure and seepage forces tending to cause such a movement.

In this formulation the numerator involves the standard equation for shear strength $s = c + (\sigma_n - u) \tan \varphi$, wherein the variables are expressed in scalar terms as values of stress or pressure. Here, these quantities are converted to forces so that the resulting items, being vectors, can be examined for closure of their force polygons.

There are two forces which contribute to the frictional resistance, these being: the effective weight of the soil column, and then, the vertical component of the Seepage Force. Similarly, the denominator is comprised of the slice forces acting to promote lateral displacement. These are the horizontal components of the Seepage Force (SF_H) and H, the horizontal component of the normal force (N). In addition to these slice forces, in some situations there can be a simple single hydrostatic influence (L) introduced into the ratio-balance by standing water at either end of the section, such as the pond or a crack on the upstream side, &/or tailwater on the d/s side.

The Factor of Safety by this h-method is therefore calculated =

$$\frac{\Sigma \left[C_H + (W' + SF_V) \tan \varphi \cos^2 \beta \right]}{L + \Sigma \left[SF_H + H \right]} \qquad \text{Equation 2}$$

where, for each slice:

C_H	cohesive resistance, horizontal component
W'	effective weight of soil column
SF_V	Seepage Force, vertical component
φ	angle of frictional resistance
β	angular inclination of base
L	differential hydrostatic end forces, top minus bottom
SF_H	Seepage Force, horizontal component
H	horizontal component of normal force (N)
Σ	summation of values across all slices

The next necessary move is to compare these h-method results with those computed by a recognized and authoritative stability analysis program to see what ensues. The Janbu solution [Ref 4] for the determination of the stability of a sliding mass on a non-circular slip surfaces is the obvious choice. Both approaches use the method of slices and both assess/determine stability on the basis of horizontal equilibrium.

In order to make the comparison as simple and non-contentious as possible the following steps were taken:

1. The unit weights of the cohesive and the frictional soils made the same by setting void ratios at 0.5 for both soil types.

2. The angle of shear resistance for granular soils was set at $\varphi = 30°$. Then, by trial and error, it was established that for this section and no SFs, an equivalent strength for cohesive soils would be 2,800 lb/ft^2.

These values were subsequently adopted/used in all the analyses reported here.

Results

What is required to be known, by comparing the results of the two methods of analysis is to what extent the inclusion of SFs in the h-method differs from the standard Janbu procedure where SFs are not considered.

Three embankment sections have been chosen for analysis, these differing from each other only in regard to their phreatic surfaces, as depicted in Figures 7, 8, and 9. In addition, these three were evaluated both for the situations where the trial interface passes mainly through the cohesive soil (c.&.φ), and also where the soil is made to be entirely frictional (all.φ). The results of these six stability analyses are listed in Table 1 for both methods of analysis.

The first pairing, labeled "no pond", is for a condition where the phreatic surface is made coincident with tailwater level, as shown on Figure 7. This extreme position is most unlikely to be encountered in the field but is of interest here in that it abstracts any influence of SFs, thus providing a baseline situation against which other phreatic surfaces may be compared.

The second pairing is for the high phreatic surface shown on Figure 8, and produced the results shown on the table across from the "no drain" label, is meant to depict a natural slope of embankment where there has been no effort to control the seepage artificially. It needs to be declared that this surface was not determined from any

combination of permeability components, but rather, it was chosen simply for illustrative purposes. Here we see that there is a noteworthy difference between the FoS calculated for the two soil types.

TABLE 1 – Numerical Results of Stability Analyses

CONDITIONS		Seepage Force components		Factor of Safety		JANBU versus h-method
		Horizontal	Vertical	h-method	JANBU	[(J-h)/h]
no pond	c .&. φ	0	0	3.0	3.2	9 %
	all φ			3.0	3.1	4 %
no drain	c .&. φ	199 kips	41 kips	1.8	2.8	59 %
	all φ			1.3	1.9	42 %
chimney drain	c .&. φ	152 kips	102 kips	1.9	3.0	61 %
	all φ			1.9	2.7	42 %

The third pairing is for the low, artificially depressed, phreatic surface shown in Figure 9. The FoS results are listed in the table across from the "chimney drain" label. Both results are virtually the same at about 1.9.

Discussion of Results

Let's first look at the numbers on Table 1 which were computed by the stability analysis method advocated herein, and listed under the column heading "h-method".

With reference to Figure 7 we see that the "no pond" pair of results both give FoS = 3.0, which should come as no surprise because, as stated above, the strength parameters were manipulated to bring about this equivalence. Both SF components are zero, again a result of deciding to set the phreatic surface at tailwater level. It is gratifying to find that the Janbu results for this situation are much the same as the h-method, being computed at 3.2 and 3.1 for the c.&.φ and all.φ cases, respectively. This, I think, is a reasonably good level of agreement. Showing that the two method are in the same ballpark.

In the case of the second pairing, for the situation depicted in Figure 8, and with results listed against the label "no drain", the big difference between the c.&.φ and the all.φ needs comment. And this can be explained as follows: the high phreatic surface means that most of the overburden is buoyant and while this has little impact on the resistance of the c.&.φ section, it results in a large strength reduction in the case of the all.φ section because W' is much reduced.

What is more important to note is the very significant escalation of the differential between the two methods of analysis where the Janbu method suggests a FoS which exceeds the h-method by as much as 59% and 42% for the c.&.φ and all.φ cases, respectively. This is a serious disparity.

The third pairing, for the physical situation depicted in Figure 9, the results are listed against "chimney drain" in Table 1. The fact that the c.&.φ h-method result for the "chimney drain" didn't show much improvement over the equivalent value for the "no drain" situation came as a bit of an unpleasant surprise for me since I favor this design approach. Nevertheless, I suppose that I can still take some consolation in knowing that this type of drain removes concerns about differential horizontal-to-vertical shell permeability which could result in seepage breakout on the downstream slope face. The differential between the two methods of analysis where the Janbu method suggests a FoS which exceeds the h-method by as much as 61% and 42% for the c.&.φ and all.φ cases, respectively.

Since now we are dealing with the same embankment sections, phreatic surfaces, soil strength parameters, and unit weights, we must let the computed FoS from each procedure speak for themselves.

The above comparisons show that treating the seepage water within a slope as a matter of hydrodynamics, which it truly is, yields FoS values far lower than those which are arrived at when seepage is dealt with as a hydrostatic condition. In consequence, it must be concluded that our standard formulations of stability analyses which deal in terms of pore water pressures, rather than seepage forces, err significantly on the unsafe side.

CONCLUDING REMARKS

It is a mistake to treat saturated soil as a fixed entity. Such, it is not. Saturated soil is a two-phase material where the two phases are not locked together, they do not necessarily act in concert. The water is entirely free to move within the soil-structure, but can only avail itself of this freedom of relocation when/while it has the energy to do so. This is because water must expend energy to do the work entailed in overcoming the drag resistance the soil-structure puts in the way of such relative motion between the phases.

Hydraulic head, as depicted by the phreatic surface, is a measure of the available energy in the water. Hydrodynamic energy is available to the liquid phase whenever/wherever it finds itself under the dominion of a hydraulic gradient. Where there is no hydraulic gradient the situation is hydrostatic: The water cannot move. Therefore, other than by buoyant effect, the pore water has no power to affect the soil-structure. Seepage Force is a convenient way to quantify the particular work-energy equation in governance here.

There is a demonstrable need, as shown here, to upgrade the way in which the geotechnical community currently assesses the stability of natural slopes and earthfills subject to seepage flow, such as embankment dams or tailings dams.

One must surely wonder why, given the prevalence and power of SF in earthdams and other embankments subject to seepage flows that their presence has apparently not been the subject of serious concern/treatment. As long ago as 1948 Donald W Taylor of MIT introduced the concept of SF, see Ref 5. More recently (50 years later) the idea was appealed to in 1998, see Ref 6. But it never seems to have gained traction in the world of geotechnical engineering.

I can only imagine that this oversight was because of some subliminal association between flow velocity and SF, simply because D'Arcy's Law for rate of fluid flow through a porous medium ($v = i\,k$) and Taylor's equation for SF both contain hydraulic gradient (i) as the independent variable. It would follow (mistakenly) that since seepage velocity is always very slow, then SF must also be low. The fact that the velocity head, $h_v = v^2/2g$ is so miniscule [e.g. If permeability $k = 2 * 10^{-2}$ ft/sec and $i = 0.5$, h_v is $1.6\ 10^{-3}$ ft (0.019")]that it would not register on standpipe piezometers, and would only serve to add further to this misconception. The reality is that the magnitude of SF is not dependent in any way on soil permeability.

A CASE IN POINT: FORT PECK DAM

The slide that seriously damaged the all but completed Fort Peck dam on September 21st 1938, is I believe, most easily explained as follows:

This 9,000 ft long embankment dam was constructed using the hydraulic-fill technique which entailed discharging pumped silty sand slurry along the centerline: the silt fraction was contained around the axis, while the sandier fraction was formed into relative flat confinement shells on either side. The upstream [**u/s]** face was built at slopes varying from 3:1 to 5:1 (h:v), while the d/s shell was built at 8½:1, [see Ref 7].

The proposition being advanced here is that the Seepage Forces attending the progress of the hydraulic-fill method provide a ***sufficient*** explanation for all that happened that day as the embankment reached/approached the right abutment, and without the need for any further hypothesis.

Up to this juncture, as the earthfill moved across the Missouri River the supernatant water from the pumped fill had the opportunity to seep away to both side slopes, ***as well as*** from in front of the advancing embankment construction. But once the embankment came up against the rock wall of the abutment * the frontal seepage route was abruptly denied/cut off.

Figure 9: the dam "opened like a gate hinged on the east abutment"

The evidence suggests the following failure mechanics:

Once face to face with the immobile rock of the right abutment, the now entrapped seepage front, triggered a *quick* condition in the surrounding sandy fill and turned that soil it into a highly energized heavy fluid.

That concentrated hydrodynamic energy, needing to vent, and given the geometric constrains of the situation, initially took the easiest exit route - the upstream face. That side was both steeper and shorter, as well as having less resistant to shear displacement because of being partially inundated. The upstream toe was submerged since the reservoir was already being used to store some water.

The aftermath of the consequential embankment failure is shown in an aerial photograph taken shortly after the event; Figure 9. What is immediately obvious is that this appearance is not the typical geometric mess which normally follows a slope failure, where there is generally little to be seen in common with the pre-failure slope face. Here, large areas, remnants of the former geometrical aspect of the slope, have been preserved even after being wafted considerable distances.

What appears to have happened here is that this part of the upstream slope, quite literally, "had the ground swept/taken out from beneath it". The source of the energy propelling these translations can be accounted for by the seepage forces that existed in front of the advancing embankment construction. Given that momentum, it then looks as if the outer face just reclined upon the heavy fluid which had undermined it.

Because of the rather gentle/soft nature of the forces impelling the earthfill movements it was possible for large sections/slabs of the original face to survive intact; these being held together by intergranular stresses referred to as "apparent-cohesion". This phenomenon can be quite influential in such fine-grained soils once they are less than fully saturated, that is, when they exist/behave under the rules of 3-phase physics. How to quantify these stresses is explained in detail in Ref 1.

Foam trails suggest that the main mass of debris rotated clockwise after being pushed away from its original location, and that surface water was not involved in the movements.

The decision to repair the damage, and subsequently commission the dam, was certainly the right decision: Once the hydrodynamic cause of failure was spent, it was quite safe to proceed under relatively/essentially static conditions.

* The four dark circles towards the upper right of the picture are the Gate Control Structures which were founded in bedrock, and thus can be used to identify the western/outer limit of the rock face.

REFERENCES

1. *Compacted earthfill is a 3-phase material*, W.E. Hodge, Phoenix-Hodge.com, 2015 Available at https://www.phoenix-hodge.com/index.php

2. *Sandisle Study,* H.G. Gilchrist & W.E. Hodge, Golder Associates Report 782-2719G, 1979

3. *the Water in the Soil - Part 2*, Geotechnical News, W.E. Hodge, 2011

4. *XSTABL Reference Manual*, Interactive Software Designs, Version 5

5. *Fundamentals of Soil Mechanics,* D.W. Taylor, 1948

6. *Liquefiable Materials and their Treatment by Vibro-Draining,* W.E. Hodge, 1998

7. US Army Corps of Engineers, District News, Vol. 11, No. 2. 1987

8. *Non-linear Soil Mechanics*, John Atkinson, NZ Geomechanics News, 2017

APPENDIX

While on the subject of stability analyses this seems to be a suitable occasion to say a few words about the angle of friction.

Since the function operating on phi is the tangent, it is important to realize that the numerical value of tan (ø) escalates rapidly as that parameter increases. Values of the tangent function at various ø angles:

ø °	20	30	40	50	60	70	80
tan ø	0.36	0.58	0.84	1.19	1.73	2.75	5.67

Since the relationship between shear strength and effective overburden pressure is $\tau = \sigma' \tan ø$ it is important to keep in mind that the tangent function is far from proportionate: when ø = zero, tan ø is also zero; when ø = 45° tan ø = 1; and if ø were to approach 90° tan ø would approach infinity.

The following picture shows two ways (linear and modified) of presenting Mohr Coulomb failure criteria for a cohesionless soil. See Ref 8.

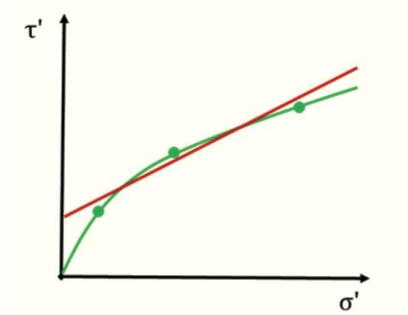

These two lines, one straight the other curved, purport to represent the locus of the frictional component of the shear strength of a non-cohesive soil mass with respect to the effective normal stress exerted on the surface being considered.

The straight line is the statistical best fit to the three data points provided by laboratory testing of the soil under examination. This line is simply misleading because the linear regression analysis from which it is derived fails to take account of the most reliable data point available, and that is the origin of the axes, where it is known that when σ′ is zero so is τ. Consequently, the linear option should not be used in geotechnical practice.

For example, if for illustrative purposes, we were to adopt the values along the curved line we would find/realize that the friction component near the axes origin is 3.17, whereas it is only 0.28 at the top extremity of the curve, a ratio of 11.4 to 1. This shows that the value of the shear strength component is highly dependent on the effective overburden pressure. The clear implication to Stability Analyses is that the slope model ought to be subdivided into zones of σ' so that appropriate friction angles may be attributed to the base of each slice along the failure surface.

END OF ESSAY

Written December 6th 2020, by:

William E Hodge (rtd M.ASCE)
Phoenix Engineering Ltd
https://www.phoenix-hodge.com/index.php

B.E. Civil Engineering (1st Hons), M.Eng.Sc. (Soil Physics)

Revision 1, December 20th 2020
Amended, March 16th 2021